

Phase synchronization analysis by assessment of the phase difference gradient

Martin Vejmelka* and Milan Paluš

Institute of Computer Science, Academy of Sciences of the Czech Republic, Praha, Czech Republic

W. T. Lee

Department of Mathematics and Statistics, University of Limerick, Limerick, Ireland

(Dated: May 8, 2009)

Phase synchronization is an important phenomenon of nonlinear dynamics and has recently received much scientific attention. In this work a method for identifying phase synchronization epochs is described which focuses on estimating the gradient of segments of the generalized phase differences between phase slips in an experimental time series. In phase synchronized systems, there should be a zero gradient of the generalized phase differences even if the systems are contaminated by noise. A method which tests if the gradient of the generalized phase difference is statistically different from zero is reported. The method has been validated by numerical studies on model systems and by comparing the results to those published previously. The method is applied to cardiorespiratory time series from a human volunteer measured in clinical settings and compared to synchrogram analysis for the same data. Potential problems with synchrogram analysis of experimental data are discussed.

PACS numbers: 05.45.Xt, 05.45.Tp, 05.45.Pq

A range of synchronization phenomena has been identified in different types of coupled complex dynamical systems. Phase synchronization is a type of synchronization reflecting mutual adjustment of rhythms of self-sustained oscillatory systems. Typically when trying to identify phase synchronization in practice, the activity of participating systems is encoded as a multivariate time series. The focus of this work is on the development of a method for detecting phase synchronized epochs in experimentally obtained bivariate time series. The criterion for identifying phase synchronized epochs is the existence of a zero gradient in the generalized phase difference of the investigated time series between phase slips. The method can be applied to phase synchronization analysis of systems studied in diverse areas of science and engineering.

I. INTRODUCTION

Synchronization, a phenomenon of cooperative behavior occurring due to interactions between complex systems, has attracted considerable interest from theoreticians as well as experimentalists (see e.g. the monograph [1]) in the last two decades. Synchronization and related phenomena have been observed in systems studied not only in physics, but also in natural and social sciences, medicine and technology. Examples include cardio-respiratory interaction [2–4], synchronization of neural signals [5–8] or episodes of synchronization be-

tween meteorological variables reflecting changes in climate [9, 10].

The strongest definition of synchronization requires that the difference between states of synchronized systems asymptotically vanishes. This definition is called *identical* synchronization [11], while the notion of *generalized* synchronization requires that states of coupled systems are (asymptotically) related by some function [12, 13]. In the case of coupled self-sustained oscillatory systems, *phase synchronization*, given by a relation of the instantaneous phases, can occur. Even a very weak coupling can result in phase synchronization while the amplitudes remain uncorrelated [14].

Some publications focusing on detecting phase synchronization in experimental data use rather qualitative methods such as the analysis of synchrograms [15]. Some authors have applied the synchrogram method to cardiorespiratory data [4, 15–17] and to brain signals [18]. Synchrogram analysis has been applied to intrinsic mode functions [17] resulting from an empirical mode decomposition [19]. The works employ visual examination of the synchrograms as a final means to decide whether the investigated systems are phase synchronized. Results based on visual examination may be difficult to reproduce and some authors have proposed numerical criteria to define “phase synchronization epochs” [16].

Other approaches advocate the use of phase synchronization indices [7, 20–22] which compute the amount of interdependence inherent in the data. Sometimes these indices are accompanied by recommendations for significance tests using surrogate data. These methods focus on detecting the existence of coupling between systems and thus identify phase synchronization in a wider sense: the test results are positive when the systems exhibit a coupling strong enough to be detected. It is however not necessary that the phases or frequencies lock for such

*Electronic address: vejmelka@cs.cas.cz

tests to report positive results.

In this work a new approach to detecting phase synchronization is proposed which focuses on the behavior of coupled systems between “phase slips”. The null hypothesis of the proposed method is that the two systems are phase synchronized and a statistical procedure is employed to test it. This is a conceptually correct construction because the alternate hypothesis is that the systems are either independent or dependent but not phase synchronized. The use of a strict null hypothesis allows for the construction of a statistical test to determine whether the data allows one to reject it at a given significance level. The performance of the method is demonstrated with numerical studies, by reproducing previously published results and on an experimental example. In practice it may be difficult to obtain segments without any phase slips for analysis and a robust regression method has been used that allows a phase slip to be present at the edge of an epoch without negatively impacting the results.

The rest of the paper is organized as follows: the next section considers phase synchronization in detail, in Sec. III the method of identifying phase synchronization epochs is introduced and Sec. IV details the numerical studies that shows the performance of the newly proposed approach. The method is applied to cardiorespiratory data measured in a clinical setting in Sec. V. The paper closes with a discussion (Sec. VI) and conclusion (Sec. VII).

II. PHASE SYNCHRONIZATION

In theory [1, 23], mathematical definitions exist to describe synchronized systems and the effect of synchronization on their phases. On the other hand in time series analysis synchronization is often interpreted as a statistical phenomenon, leading to the quantification of a “degree of synchronization”. In the following paragraphs mathematical definitions of phase synchronization are briefly recounted.

The criteria of synchronization make use of the definition of the *generalized phase difference*

$$\psi_{mn} = n\phi_1 - m\phi_2, \quad (1)$$

where $\phi_{1,2}$ are the instantaneous phases describing the motion of the two systems, ψ_{mn} is the generalized phase difference and $m:n$ is the locking ratio. In the above case, m periods of the first system (represented by ϕ_1) correspond to n periods of the second system. Where appropriate, the subscripts m, n are dropped to simplify the notation. In the rest of this paper, the term phase difference will be interchangeably used with the term generalized phase difference as $m:n$ phase synchronization is explicitly considered in this work.

The condition for phase synchronization is usually given in the form [1]

$$|\psi_{mn}| < \text{const.} \quad (2)$$

This condition is applicable to series of infinite length and would be difficult to test in practice as any finite time-series will exhibit some maximum difference whether the two systems synchronize or not. A statistical test of the absolute phase difference or a related quantity would be necessary as attempted in [24]. Another definition given in [1] is termed *frequency locking*. The condition can be stated as

$$n\langle\dot{\phi}_1\rangle = m\langle\dot{\phi}_2\rangle, \quad (3)$$

where $\langle\cdot\rangle$ denotes the time average. The same condition can also be written as

$$\langle\dot{\psi}_{mn}\rangle = 0. \quad (4)$$

In the case of deterministic dynamics the above criteria of phase synchronization are equivalent. However when the systems are disturbed by noise the situation becomes complicated. If the intensity of the noise is not high enough to perturb the two systems so that they slip against each other then the effect is only of increasing the fluctuations of the phase difference while preserving both properties (2) and (3). Of course, the bounding constant in (2) may become larger. If the intensity of the noise is higher than this threshold then it is possible that phase slips occur and the systems slip against each other by 2π radians or a multiple thereof. If the coupling between the systems is strong then the phase difference rapidly changes — “jumps”. The increase may be somewhat slower if the coupling is weak. In this regime, the phase difference is essentially unbounded and the criterion (2) cannot be fulfilled. However the mean frequencies should still be equal in this regime even though the phase difference may exhibit a random walk type behavior because of the phase slips. More importantly, if the systems are phase synchronized, then there should be no systematic drift of the phase difference between the phase slips.

It may seem that the situation of deterministic coupled systems close to the phase synchronization region is the same as that of coupled phase synchronized systems perturbed by noise. This is however not the case: in the case of deterministic sub-threshold coupled (unsynchronized) systems the generalized phase difference is not constant but drifts in one direction. This is evident from the fact that the phase difference between the two systems must progress to a point where a phase slip occurs and shifts the phase difference between the systems to a new starting point for the slow drift and the situation repeats itself.

The presence of external disturbances and noise sources in many real systems makes it difficult to experimentally observe perfect phase or frequency locking (3). More frequent is the observation of *imperfect phase synchronization* [25–27], where phase synchronization epochs are intermingled with phase slips. Systems with broadband spectra and especially those with unbounded return times, such as the Lorenz system, can also slip against a driving force or against the system

to which they are coupled when they visit a particular region in their state space [25, 26]. Their phase locking behavior is described by a multi-well potential and sufficiently strong perturbations can cause the system to move from one potential well to another one [23, 28]. Even in this case the situation can be described in terms of regions between phase slips: for sub-threshold coupled systems, the phase difference between phase slips is not constant but systematically drifts.

III. PHASE SYNCHRONIZATION ANALYSIS BY GRADIENT ESTIMATION

In this section an approach to detecting phase synchronized epochs based on the above considerations is described. Following our previous line of thought a test must be constructed to determine if the gradient of the phase differences of the analyzed segment is statistically different from zero. If the phase difference time series constructed using (1) does not contain phase slips then a suitably long segment can be used according to results from numerical studies and the analysis can be split into multiple epochs as needed.

There are some important practical issues: one is that of fluctuations. Some fluctuations can be so large that they can obscure a small trend in the evolution of the phase differences. This may happen if there are very large fluctuations or if the trend is almost negligible (on the border of the synchronization region). The second issue is the selection of segments not containing phase slips: in practice it may be difficult to select analysis segments so that they do not contain any phase slips. The proposed gradient estimation method can cope with a phase slip near the edge of an analysis epoch by using a robust estimation method.

The hypothesis test that will be constructed assumes that the gradient is zero the phase difference time series and tries to use the evidence in the time series to reject it. The problem is that the statistical distribution of the gradient is unknown and the test must be devised so that its significance can be tested using another method.

To estimate the gradient in the data we use least squares linear regression

$$\psi(i) = at(i) + b + \delta(i), \quad (5)$$

where ψ is the generalized phase difference and a , b are chosen to minimize $\chi^2 = \sum \delta(i)^2$ [29, 30]. As a corollary to this we have that mean $\delta(i)$ is zero. Subtracting the equations for $\psi(i)$ from the equation for $\psi(i+1)$ and rearranging gives

$$\frac{\psi(i+1) - \psi(i)}{t(i+1) - t(i)} = a + \frac{\delta(i+1) - \delta(i)}{t(i+1) - t(i)}. \quad (6)$$

Averaging over all samples and taking the limit $t(i+1) - t(i) \rightarrow 0$ gives

$$\langle \dot{\psi} \rangle = a. \quad (7)$$

Independently of the actual (complicated) evolution of the phase difference a linear trend will be present if the phase difference drifts systematically. In experimentally obtained time series, noise and fluctuations will invariably cause the value of a to be slightly different from zero. The question remains whether the gradient a is significantly different from zero.

The key difficulty with this approach is that the statistical properties of the time series are not known. Phase synchronization detection methods are often applied to complex systems whose physics are poorly understood. Often the only statistical information available is that contained within the time series themselves. This leads us to the following idea: a horizontal line is fitted to the time series using the same approach as previously and errors of the two fits are compared. The equation for a horizontal line is simply

$$\psi(i) = c + \eta(i), \quad (8)$$

where $\eta(i)$ are the fit errors. The least squares fit is just the arithmetic average $c = \langle \psi(i) \rangle$. Using a least squares fit ensures that $\langle \eta(i) \rangle = 0$. We stress that it is not critical that ordinary least squares regression is used. The estimator is only required to guarantee that the residuals $\{\delta(i)\}$ and $\{\eta(i)\}$ will have zero means, otherwise the gradient estimate will be biased.

If the two systems are phase synchronized then there is no real gradient and the value of a extracted from the linear fit is just a random fluctuation about 0. This means that the residuals $\{\delta(i)\}$ and $\{\eta(i)\}$ are drawn from the same distribution and, because of the non-zero value of a , one of the datasets is slightly perturbed. On the other hand, if there is a significant gradient in the $\{\psi(i)\}$ then the datasets $\{\delta(i)\}$ and $\{\eta(i)\}$ will belong to different distributions.

There is a standard test to verify if two datasets have been drawn from the same distribution — the Kolmogorov-Smirnov test [29, 31]. The test computes the probability that the maximum difference in the cumulative distribution functions estimated from two samples will be observed, assuming that they are drawn from the same probability distribution [29]. The test makes no assumptions about the nature of the underlying distribution and is invariant under a re-parameterization of the data. In this work we characterize a time series as unsynchronized if the Kolmogorov-Smirnov test gives a probability of less than 5% that the residuals $\{\delta(i)\}$ and $\{\eta(i)\}$ are taken from the same probability distribution.

Long-term correlations in the phase difference time series can cause spurious rejections of the null hypothesis as sometimes they are detected as a trend. In applications to experimental data, it is likely that measurement error will be a further source of fluctuations. Our approach to reduce the problem is to sort the time indices by the associated phase differences. The input to the transformation is a set of pairs $(\psi(i))_{i=1}^N$. A sequence of indices $J = j_1, \dots, j_N$ is computed such that the sequence $(\psi(j_i))_{i=1}^N$ is sorted in ascending order. Now the in-

dices j_i define a new order on the data points so that $\psi(i)$ will be at the j_i -th position. Many software libraries contain the function `argsort` which can be used to obtain J as $J = \text{argsort}((\psi(i))_{i=1}^N)$. If the phase difference series contains a trend, the sort will entail “local” mixing only and the autocorrelation function of the phase difference time series is not appreciably changed [41]. If, on the other hand, there is no long-term trend then the series is “globally” mixed thereby significantly attenuating the magnitude and cyclicity of the autocorrelation function. This is exactly what is required to reduce the influence of the correlations on the quality of the least squares fit. This procedure causes slightly higher false positives when series with a high noise content are analyzed. Excessive noise may obscure the trend in the phase difference time series which then becomes difficult to detect. Nevertheless, the amount of data required for accurate detection is dramatically reduced and the method becomes highly effective. The above procedure improves the effectiveness of the method considerably and that is the only reason of its inclusion in the method.

In numerical experiments the above approach is very effective. Experimentally obtained data is frequently partially contaminated by outliers (such as phase slips or measurement errors) and noise. These may adversely affect the estimation of the generalized phase difference gradient. Thus in practice a more robust approach to fitting the straight line (5) of the generalized phase differences is in order. Least trimmed squares (LTS) regression [32] is particularly suited to this task as the estimator starts out with the hypothesis that a subset of the data are outliers. The LTS approach proceeds by assuming that at least h data points out of the total of N analyzed are leverage points (useful data) and the rest are outlier points. Given this assumption an algorithm such as FAST-LTS [33] can be applied to find this subset and estimate the fit parameters. In the numerical examples the dependence of the sensitivity and specificity on the parameter h is examined. The minimum value for h is $N/2 + 1$ which yields an estimator with the highest possible breakdown point, a measure of the robustness of the fit. Related approaches such as Least median of squares are not suitable as the mean of the errors is not guaranteed to be zero which is required by the analysis above. When LTS is applied the mean (8) is calculated from the set of points selected as leverage points by the LTS method when fitting the straight line (5) so that the distributions of the errors come from the same set of points and are comparable.

The method above is one way of statistically testing the gradient of the phase difference time series against a null hypothesis of zero gradient. It takes into account the fact that the statistical properties of the gradient estimate are unknown and that a subset of the time series may not represent useful information. This happens if a phase slip is at one of the edges of the analyzed segment.

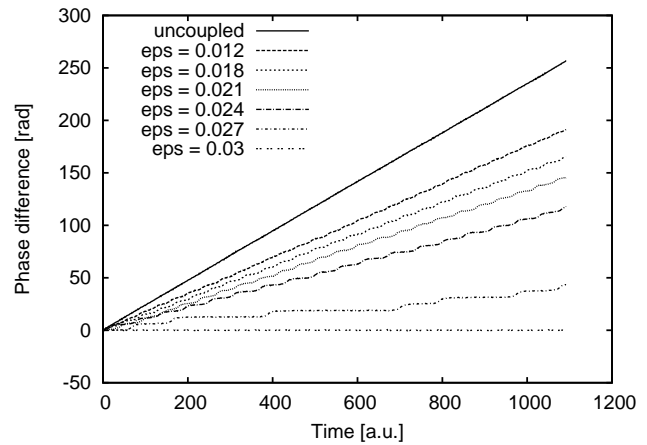


FIG. 1: Evolution of the phase differences for different strengths of coupling C from a pair of symmetrically coupled Rössler oscillators (9).

IV. NUMERICAL STUDIES

Detailed numerical experiments have been performed on the paradigmatic pair of symmetrically coupled Rössler systems to investigate the behavior of the proposed method. The equations of a symmetrically coupled Rössler oscillator pair can be written as

$$\begin{aligned} \dot{x}_{1,2} &= -\omega_{1,2}y_{1,2} - z_{1,2} + C(x_{2,1} - x_{1,2}) \\ \dot{y}_{1,2} &= \omega_{1,2}x_{1,2} + 0.15y_{1,2} \\ \dot{z}_{1,2} &= 0.2 + z_{1,2}(x_{1,2} - 10), \end{aligned} \quad (9)$$

where $\omega_{1,2}$ controls the frequency of the oscillators and C represents the strength of coupling. The behavior of symmetrically coupled Rössler oscillators has been thoroughly investigated [1, 14, 28, 34, 35] and is well understood. The evolution of phase differences with respect to coupling strength is emphasized and shown in Fig 1. It is clear from the figure that an almost linear evolution of phase differences persists until approximately $C = 0.027$ where “plateaus” appear interspersed with phase slips. However these “plateaus” are not segments with zero phase difference gradient, they only appear so because the growth of the phase difference is small. At the transition to synchronization there is a relationship between the frequency of phase slips and the difference between a given coupling strength and the synchronization threshold [35, 36]

$$N_s \sim \exp|C - C_t|^{-1/2}, \quad (10)$$

where $C_t = 0.03$ is the synchronization threshold, C is the strength of symmetrical coupling in (9) and N_s is the number of slips per unit of time. When the synchronization threshold is reached, the systems synchronize and the phase difference remains within tight bounds. For reference the phase difference evolution for the uncoupled systems is also shown (top curve in Fig. 1): clearly the systems are unsynchronized for $C \leq 0.024$ and their

relative phase velocity is more than half of the relative phase velocity of the uncoupled systems.

A Runge-Kutta 4th order scheme was used to integrate the oscillators with a step of 0.01 s, the resulting time series was sub-sampled by a factor of 10 to yield a time series with approximately 60 points per period. The phase extraction procedure is similar to the one used in [34]: projecting the attractor into a plane spanned by two selected coordinates and using the angle of the line from the origin to the current position of the system state in this plane as the instantaneous phase. The period of the oscillator was first estimated by detecting the number of positive-going zero crossings and relating it to the length of the time series. This is a coarse detection of the approximate number of samples per period and corresponds to marked events phase extraction [35, 37]. Using this estimate a two-dimensional time delay embedding [38, 39] is constructed using two samples of the same time series one quarter of the estimated period apart. This separation would give an optimal projection for a harmonic oscillator. The instantaneous phase is estimated as

$$\phi(i) = \arctan\left(\frac{x(i)}{x(i - \lfloor T/4 \rfloor)}\right), \quad (11)$$

where T is the estimated number of samples per period. This is a realistic procedure and can be applied to experimental time series if it does not contain excessive noise and if the period of oscillation is relatively stable.

Fig. 2 (top) shows how the proposed method detects synchronized states in a time series originating from a pair of coupled Rössler systems for different system parameters. The plot shows the detection rates for each parameter combination: the frequency mismatch $\Delta\omega$ and the coupling strength C . The frequencies of the Rössler oscillators were derived from the frequency mismatch as $\omega_{1,2} = 1 \pm \Delta\omega$. The number of samples used as input to the detection method is 1024, which represents approximately 18 periods. The image can be directly compared to Fig. 2 (bottom) which appeared in the work of Rosenblum et al. [14]. The figure shows the computed mean frequency mismatch $\Delta\Omega = |\langle \dot{\phi}_1 \rangle - \langle \dot{\phi}_2 \rangle|$ for the same parameter range. The systems are considered synchronized if $\Delta\Omega$ is negligible. The results of the proposed detection algorithm are clearly in agreement with previously published results. The detection rates are close to 0 in the unsynchronized region and close to 1 in the synchronized region.

In Fig. 3 the results for a pair of symmetrically coupled Rössler systems with $\omega_{1,2} = 1 \pm 0.015$ are shown. The experiment was run for all coupling strengths $C \in (0, 0.04)$ with a step of 0.002. Only relevant parts of the results are shown as for $C < 0.024$ the detection rates are negligible and for $C > 0.34$ they are close to 1. The plot shows how the parameter h indicating the assumed number of leverage points inside the dataset affects the detection statistics. For $h = N/2 + 1$ it is clear that some sensitivity is lost and for $h = \frac{3}{4}N$ the results are very close to those for $h = N$. In this numerical example there

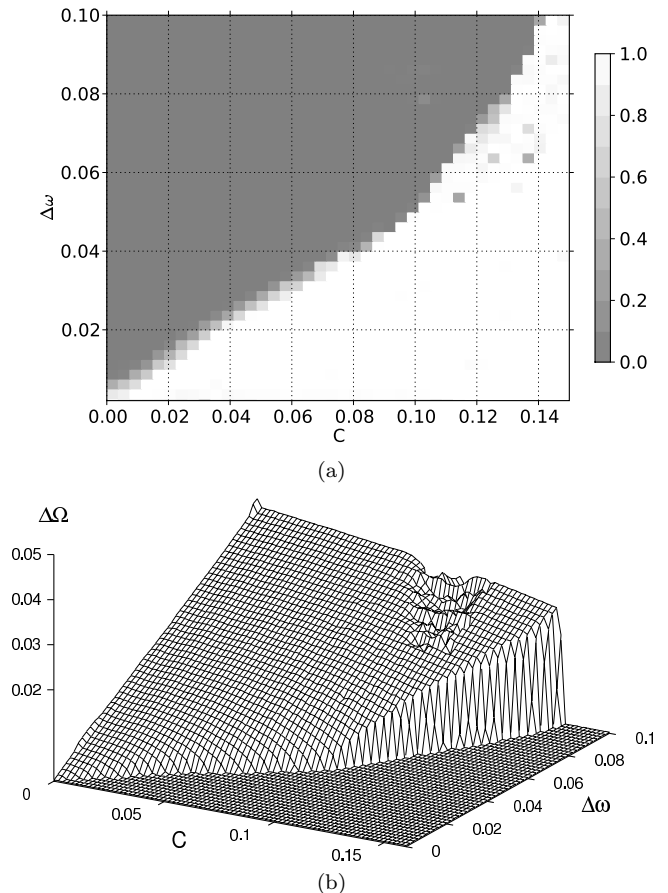


FIG. 2: Detection rates for the proposed method using Least trimmed squares ($h = \frac{3}{4}N$) from short time series of ≈ 18 periods (a) and difference of mean frequencies for a symmetrically coupled Rössler system pair (b) from [14], used with permission. C represents the coupling strength, $\Delta\omega$ represents the nominal frequency mismatch and $\Delta\Omega$ is the actual frequency difference computed from the time series. The systems are considered synchronized when the computed frequency difference $\Delta\Omega$ is negligible. In this region, the detection rates are close to 1 almost everywhere.

are no outliers, so setting $h = N$ is optimal and makes use of all the data. However using three-quarters of the available points has not diminished the performance of the detector significantly (cf. Fig. 3, compare center and right plot). This is the value of h that will be used in the analysis of cardio-respiratory synchronization in the next section. This will allow the existence of phase slips at the edge of the analyzed segments.

There are some positive detections for the coupling $C < 0.028$ for shorter windows. This is because the amount of variability (although deterministic in the model systems) is too high for the very small gradient to be detected in short time series. In the numerical experiments such false positive classifications happen more often in short time series (cf. Fig. 3) and only just before

the phase synchronization threshold. This corresponds to previous considerations in Sec. III on high noise content obscuring a small gradient.

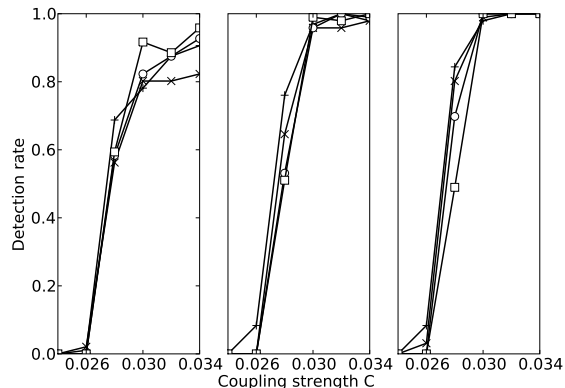


FIG. 3: Results of the proposed method for symmetrically coupled Rössler oscillators: detection rates for Least trimmed squares estimation with $h = N/2 + 1$ (left), $h = \frac{3}{4}N$ (center) and ordinary least squares estimation, $h = N$ (right). Epoch lengths: 34 periods (pluses), 68 periods (crosses), 136 periods (circles) and 273 periods (squares).

V. APPLICATION TO CARDIO-RESPIRATORY DATA

The analyzed ECG (electrocardiogram) and respiratory effort time series have been acquired in the context of the EC FP6 BRACCIA project. Measurements were carried out in the waking state and under general anesthesia for spontaneous or controlled respiration depending on the choice of anesthetic for the subject. The aim was to obtain a record of about 20–30 minutes of the activity of the heart and lungs in each state. In this first study only subjects with no neurological or degenerative diseases and with no cardiovascular complications were included. Subjects that have agreed to provide data to the project were lying still while the recording in the waking state took place. For the analyzed subject general anesthesia was induced with Sevoflurane (an inhalatory anesthetic) and the neuromuscular blocking agent Cis-atracurium (also known as Curare) was administered. The subject had to be provided with a breathing apparatus, which provided forced periodic drive to the respiratory system.

The observed time series were preprocessed to extract peaks and obtain a linearly interpolated phase time series. The ECG time series was filtered with a high-pass filter to remove baseline fluctuations, R-peaks were detected using an ad-hoc approach and the results were visually checked. The respiratory time series was band-pass filtered to smooth the waveform and remove various artefacts and low-frequency baseline fluctuations. Then the time instances of local maxima were extracted. In

both cases the peak times t_k were used to construct an interpolated phase time series

$$\phi(t) = 2\pi \frac{t - t_k}{t_{k+1} - t_k},$$

for $t_k \leq t < t_{k+1}$. The phase time series was subsampled to 60Hz from the original 1200Hz sampling frequency and the analysis was performed by a moving window strategy with windows of 8192 points (≈ 136 seconds) with no overlap. The main concern here is that in one window, there should be as many data points as possible but only one segment between phase slips should be analyzed. If the window contains two different segments separated by a phase slip in the middle, then the method will not be able to compute the gradient of either segment: the returned value will be an estimate of the gradient of the larger segment perturbed by the data points from the smaller segment. Such a result is not meaningful for our purposes. Using 8192 points we have been able to fulfill this requirement of having a dominant segment in each window. Otherwise a more sophisticated approach with manual selection of segments between phase slips would have to be employed.

The proposed method was configured to be used with interpolated phase time series from peak detection methods. Of crucial importance is an estimate of the number of independent data points. Numerical experiments have shown that for phase time series derived from the simple embedding approach it is sufficient to take the number of data points as the number of independent samples although this is clearly not the case. For interpolated phase time series the number of independent measurements is bounded from above by the number of periods. In numerical experiments not reported in this work it was sufficient to use the number of periods as the number of independent measurements in the Kolmogorov-Smirnov test. The same has been used here: for each analyzed epoch, the number of periods was found for both time series and passed into the Kolmogorov-Smirnov two sample test (cf. Sec. III).

The detection of phase synchronized epochs was based on two steps. The first was the estimation of the rational frequency ratios of the two systems. The mean frequency ratio was computed in each epoch and matched with the closest ratio of integers where the number of respiratory periods was fixed at 1, 2, or 3 per N heartbeats. The choice was thus constrained to $m:n$ with $m \in \{1, 2, 3\}$ and n an integer. For the closest ratio (e.g. 3:14, 2:15 or 1:4) in each epoch, the proposed method for identifying phase synchronization was applied to the generalized phase difference. The best fitting integer ratio is by itself important and was also used (a-posteriori) in the construction of appropriate synchrograms and phase difference plots for the awake state and anesthetized state. It was found that the simple estimator of the frequency ratio

$$f = \frac{\langle \Delta \phi_{\text{card}}(t) \rangle}{\langle \Delta \phi_{\text{resp}}(t) \rangle}, \quad (12)$$

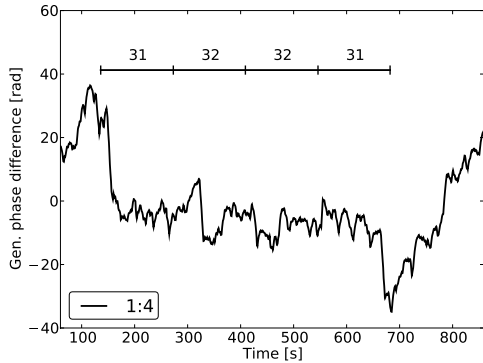


FIG. 4: Generalized phase difference 1:4 for the cardiorespiratory system of the subject in the awake state, resting. Thick horizontal line indicates epochs detected as phase synchronized. The markers show window edges and the number of respiratory periods in each epoch is given.

was misled by any phase slips or acquisition errors in the analyzed epoch. Therefore the more robust LTS estimate of the mean frequencies was applied to yield

$$f_{LTS} = \frac{\langle \Delta\phi_{\text{card}}(t) \rangle_{LTS}}{\langle \Delta\phi_{\text{resp}}(t) \rangle_{LTS}}, \quad (13)$$

where $h = N/2 + 1$ points were used to compute the robust estimate of the mean. The effect of phase slips was thus excluded from the estimate of the frequency ratio.

In the awake state, strong cardio-respiratory phase locking was found at a ratio of 1:4. Here both of the participating systems can be considered autonomous oscillators and the interaction can be analyzed in the framework of phase synchronization. The strength of the mutual locking is apparent from the generalized phase difference plot in Fig. 4 where the phase difference

$$\psi_{1:4}(t) = 4\phi_{\text{resp}}(t) - \phi_{\text{card}}(t)$$

is constrained within a 20 rad region for more than 9 minutes. However even close examination of the synchrogram in Fig. 5 does not seem to reflect this. The phase synchronization detector clearly indicates the correct epochs of synchronization indicated by a thick horizontal line in Fig. 4. Phase locking has been found in the subject in the awake state which is not visible on the synchrogram but is detected by the proposed method. The reason why the phase locking episode is not visible in the synchrogram is analyzed in detail in the Appendix.

In the anesthetized state the subject was mechanically respirated using an external device generating a periodic breathing pattern. The mechanical respirator acted as a non-autonomous external force which through its action on the respiratory system influenced the cardiac rhythm. The heart, an autonomous oscillatory system, was coupled to an external periodic force and the framework of phase dynamics could be applied. The cardiac rhythm

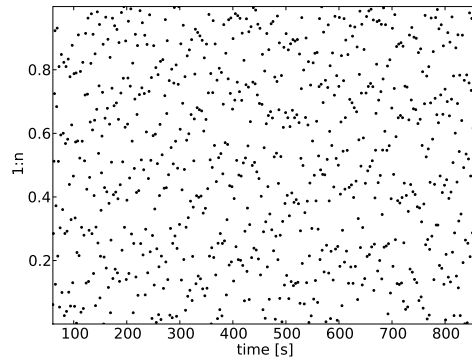


FIG. 5: Synchrogram (1:n) of the cardiorespiratory activity of the subject in the awake state.

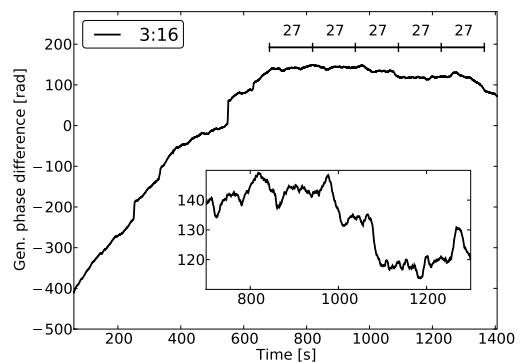


FIG. 6: Generalized phase difference ($m=3, n=16$) for the cardiorespiratory system of the subject in the anesthetized state. The markers show window edges and the number of respiratory periods in each epoch is given. Inset shows detail of segment 700s–1300s.

phase-locked to the periodic forcing strongly during the second half of the recording at a ratio of 3 respiratory periods to 16 heartbeats. The evolution of the generalized phase difference

$$\psi_{3:16}(t) = 16\phi_{\text{resp}}(t) - 3\phi_{\text{card}}(t)$$

is shown in Fig. 6. The plateau from about 700s to 1300s is clearly visible and a detailed view is in the inset of Fig. 6. This synchronization can be seen also in the synchrogram in the same time frame (Fig. 7). In the segment where the phase difference plateau is located the proposed method has correctly identified coupling in all epochs. Synchrogram analysis and the proposed phase synchronization identification method agree well in this instance.

VI. DISCUSSION

Theoretically, synchronization is a process, not a state [1]. The only way to reliably detect whether synchroniza-

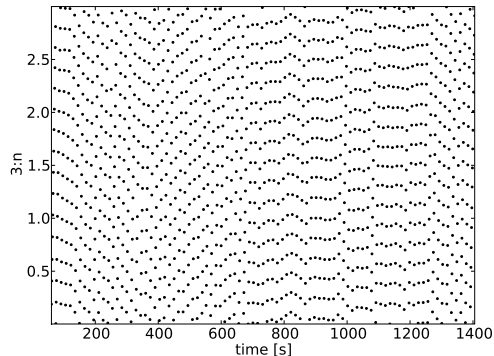


FIG. 7: Synchrogram (3:n) for the cardiorespiratory system of the subject in the anesthetized state.

tion is taking place is to perform an *active* experiment, i.e. to introduce a disturbance into the coupled system and observe whether a phase locked state is reasserted once the transient effects disappear. In principle, it is not possible to detect with certainty whether two systems are synchronized purely from their time series recorded in a passive experiment. It is however possible to statistically test whether the time series reflect a *synchronized state* as per the definitions (2) and (3). Of course a state satisfying these mathematical conditions can come about due to other effects than synchronization and this would result in a false positive detection. Assumptions about the detector and the time series must be carefully reviewed and only if they are satisfied can the result of the detection be considered valid.

VII. CONCLUSION

A new approach to the problem of detection of phase-synchronized states has been proposed. The method is based on the analysis of the phase differences gradient. A zero gradient indicates a phase synchronized epoch of the coupled systems. This is a principled way to detect phase synchronization even in the presence of noise. A test which detects if the gradient of the phase differences is statistically different from zero has been constructed. The test ensures that only phase synchronized states are identified as such, while states where the coupling is not strong enough to ensure locking of frequencies and phases are excluded. The test uses robust statistics so that analyzed segments may contain phase slips at their edges without negatively impacting the results of the estimation.

The proposed method has been shown to be effective in detecting phase synchronization in the paradigmatic Rössler oscillators. Furthermore, our tests show that the method is capable of distinguishing between synchronized and unsynchronized states using a relatively small sample of data.

The method has been applied to cardio-respiratory data acquired in a clinical setting. Data from a subject exhibiting strong cardio-respiratory synchronization in the awake state and cardiac phase locking onto a periodic force in the anesthetized state was analyzed. The results of the method have been compared with generalized phase difference plots and with synchrogram analysis. It was shown that the proposed method detects synchronization epochs in the data even when a synchrogram might not indicate phase synchronized segments. Some caveats when using synchrograms and simple safeguards against these were described in the appendix.

VIII. ACKNOWLEDGMENTS

This work was supported in part by the European Commission 6th Framework Programme project BRACCIA (Contract No 517133 NEST) and by the Institutional Research Plan AV0Z10300504. Some of the computations were performed using supercomputing resources in the Edinburgh Parallel Computing Center within the framework HPC-EUROPA (RII3-CT-2003-506079). We gratefully acknowledge the work of Tomas Draegni, Per Kvandal, Svein Landsverk and Johan Raeder in acquiring the data within the scope of the BRACCIA project.

Appendix: Synchrogram analysis

We analyze in detail why the synchrogram in Fig. 5 does not clearly indicate phase synchronization although a genuine phase difference restraint is evident in Fig. 4. To illustrate the issue, we will visualize additional information pertaining to the synchrogram plot.

If two deterministic systems are phase synchronized in an $m:n$ regime, we expect that n periods of one system correspond to m periods of the other system. As a convention $m \leq n$ and we will assume this here without loss of generality. If the systems are perturbed by noise, the situation is more complicated and the number n of periods of the faster system in m periods of the slower system fluctuate as sometimes the systems evolve apart slightly but must return back if the generalized phase difference is genuinely restrained. Let us concentrate on the faster system: if it's activity is transiently faster, then there will be in m periods of the slower system $n^* > n$ periods of the faster system and vice-versa. On average the relationship of n periods of the faster system (heartbeats in our case) to m periods of the slower system (respiratory cycles) should hold. If and only if the faster system consistently has $n^* > n$ periods or consistently has $n^* < n$ periods per m periods of the slower system can there be any systematic increase or decrease of the generalized phase difference (for a detection method based on similar considerations cf. Quiroga et al. [40]). We will exploit this fact in the following considerations.

In Fig. 8 the number of heartbeats inside each respiratory period of the awake patient fluctuates around 4 (corresponding to the 1:4 synchronization) and the average for the whole segment is exactly 4. The situation for the anesthetized patient in Fig. 9 clearly changes at about 730s into the recording. In the first part, the number of heartbeats n per 3 respiratory periods is consistently either 16 or lower than 16. This means that there cannot be a 3:16 synchronization and the generalized phase difference $\psi_{3:16}$ in Fig. 6 consistently increases. In the second part of the recording the number of heartbeats clearly fluctuates around 16 and is often exactly 16.

We now draw a parallel between the situation in the right half of Fig. 9 and in the whole of Fig. 8. On a macroscopic level (in terms of entire respiratory periods), there is no evident systematic increase or decrease and thus the results reflect the tendency of the generalized phase differences in Figs. 4 and 6 (synchronized region only) showing the generalized phase differences which fluctuate (strongly in the awake case, weakly in the anesthetized case) but does not systematically deviate in either direction.

Turning our attention back to the synchrograms, we will now explain why in the awake case the phase synchronization is not evident while in the anesthetized case it is. To do this, we will track what happens to every n -th heartbeat in the recording. Our reasoning is the following: if the systems are not synchronized and the generalized phase difference is systematically increasing

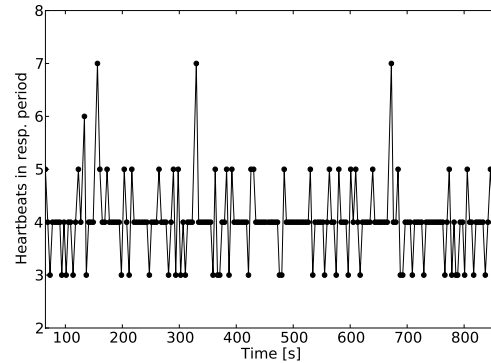


FIG. 8: Plot of number of heartbeats in each single respiratory period for the awake patient (corresponds to synchrogram in Fig.5).

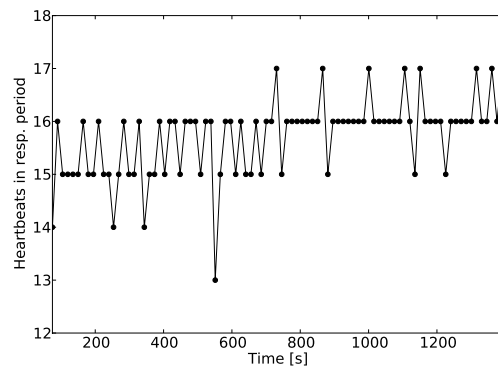


FIG. 9: Plot of number of heartbeats in each respiratory period for the asleep patient (corresponds to synchrogram in Fig.7).

or decreasing, we will see a consistent vertical drift across the synchrogram of the sequence of every n -th heartbeat. If the systems were perfectly synchronized the n -th heartbeat would show up at approximately the same position all the time. The synchrograms depicting a phase synchronized regime can be influenced by mild fluctuation as in Fig. 7 or by strong fluctuation as in Fig. 5.

We will now assume that a synchrogram depicts a phase synchronized pair of systems. In the case of small fluctuations which permit the “rows” of points to be clearly separated, phase synchronization can be identified by means of a synchrogram visually. If the fluctuations are strong so that these rows overlap or even the order of heartbeats in each period is changed, then the standard synchrogram cannot be used to identify the synchronization. This is exactly what has occurred in the case of the patient in the awake state.

The synchronization is 1:4 in the awake case and we will thus connect every 4th heartbeat with a line and show the result compared with a standard synchrogram view. Our detailed analysis will require that the bound-

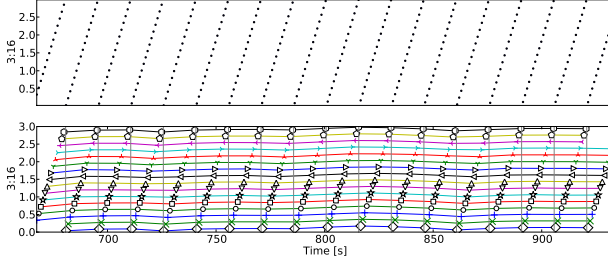


FIG. 10: Plot of the evolution of the sequences of every 16th heartbeat of the anesthetized patient in the same coordinates as a standard synchrogram plot (synchrogram is an excerpt from synchronized segment, cf. Fig.7). The fluctuations are very small and there is no apparent drift of the sequences.

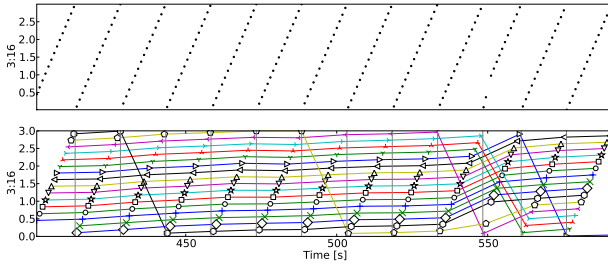


FIG. 11: Plot of the evolution of the sequences of every 16th heartbeat of the anesthetized patient in the same coordinates as a standard synchrogram plot (synchrogram is an excerpt from non-synchronized segment cf. Fig.7). The fluctuations are very small and a drift toward the top of the synchrogram can be seen.

aries of every m respiratory periods are also indicated in the synchrogram. The two synchrograms (for the synchronized and unsynchronized region) for the awake patient are shown in Figs. 10 and 11 and the same for the anesthetized patient is shown in Figs. 12 and 13.

In Fig. 10 showing the structure of the synchrogram for the anesthetized state, the lines connecting every 16th heartbeat do not overlap: the fluctuations are small. On the other hand in the awake state, the fluctuations are much stronger as is clear from Fig. 12 but note that the final state of the selected segment is identical to the starting point. This subsegment has been deliberately selected for illustration purposes but from the computations above (indicating an average of exactly 4 heartbeats per respiratory period) we know that this is the case for the entire phase synchronized segment of the awake patient which is too long to show in detail. The rows overlap and even the order of the n -th heartbeat sequences inside each respiratory period is changed on occasion. However note that the order is then changed back after some time and there is no systematic drift. As a control, the same detailed view is also shown in Fig. 11 for the epoch not exhibiting 3:16 synchronization in the anesthetized patient. Here the synchrogram resembles the synchro-

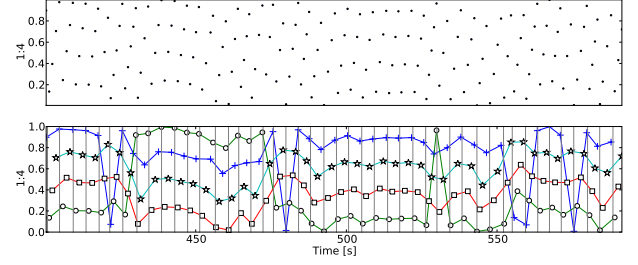


FIG. 12: Plot of the evolution of sequences of every 4th heartbeat of the awake patient in the same coordinates as a standard synchrogram plot (synchrogram is excerpt from synchronized region in Fig.5). There is no apparent drift of the sequences but large fluctuations can be seen.

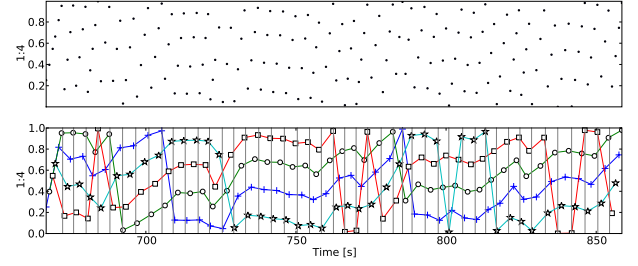


FIG. 13: Plot of the evolution of sequences of every 4th heartbeat of the awake patient in the same coordinates as a standard synchrogram plot (synchrogram is an excerpt from non-synchronized segment cf. Fig.5). The sequences clearly drift towards the top, even though the fluctuations are large.

gram for the phase synchronized region in Fig. 10 but this is because of the proportions of the figures. A direct comparison between the two regions can be made in Fig. 7. The “enriched” view of the synchrogram is however markedly different: the rows are now not horizontal but they drift toward the top of the synchrogram in Fig. 11. We stress that the above analysis is possible because we have a-priori selected a particular synchronization ratio (3:16 or 1:4) and thus have been able to assign special meaning to every n -th (16th, 4th) heartbeat and add new information to the synchrogram in the form of boundaries between every m respiratory periods and connections between n -th heartbeats.

Putting all of the ideas and results in the previous paragraphs together, it should now be clear why phase synchronization (which is genuine according to Figs. 8 and 4) in the awake state is not visible in the synchrogram. The phase differences fluctuate too much to be visually detected in the synchrogram: this is made clear by the more detailed synchrogram in Fig. 12. The standard synchrogram view of the unsynchronized segment of the awake patient in Fig. 13 is very similar but connecting every 4th heartbeat and showing their progression in different colors clearly shows the difference in the information presented in the synchrogram. In the

synchrogram corresponding to the anesthetized patient in Fig. 10 the phase synchronization is clear because there is less fluctuation in the generalized phase differences. Note that this is consistent with the result that heart rate variability and respiratory rate variability are lower under general anesthesia than in the awake state. For the analyzed patient, the interval between heartbeats in the awake state was 1.06 ± 0.14 s and in the anesthetized state 0.95 ± 0.05 s. The respiratory interval was 4.22 ± 0.54 s in the awake state and 4.99 ± 0.15 s in the anesthetized state. The variability was thus about three times smaller in the anesthetized state with the heartbeat slightly faster and

the respiration slower.

In the appendix we have tried to clarify potential pitfalls when using a synchrogram as a means of identifying phase synchronization. We have extracted additional information from the data available when creating the synchrogram and have shown that it is possible that a phase synchronization epoch is not visible in a synchrogram if strong fluctuations are present. It is not difficult to compute and plot this additional information and we suggest that this new information is added to synchrograms as a matter of routine.

-
- [1] A. S. Pikovsky, M. G. Rosenblum, and J. Kurths, *Synchronization: A Universal Concept in Nonlinear Sciences (Cambridge Nonlinear Science Series)* (Cambridge University Press, Cambridge, 2001), ISBN 052153352X.
- [2] C. Schäfer, M. G. Rosenblum, J. Kurths, and H.-H. Abel, *Nature* **392**, 239 (1998).
- [3] M. Paluš and D. Hoyer, *IEEE Eng. Med. Biol. Mag.* **17**, 40 (1998).
- [4] M. Bračić Lotrič and A. Stefanovska, *Physica A* **283**, 451 (2000).
- [5] S. J. Schiff, P. So, T. Chang, R. E. Burke, and T. Sauer, *Phys. Rev. E* **54**, 6708 (1996).
- [6] M. Le Van Quyen, J. Martinerie, C. Adam, and F. J. Varela, *Physica D* **127**, 250 (1999).
- [7] P. Tass, M. G. Rosenblum, J. Weule, J. Kurths, A. S. Pikovsky, J. Volkmann, A. Schnitzler, and H.-J. Freund, *Phys. Rev. Lett.* **81**, 3291 (1998).
- [8] M. Paluš, V. Komárek, Z. Hrnčíř, and K. Štěrbová, *Phys. Rev. E* **63**, 046211 (2001).
- [9] D. Maraun and J. Kurths, *Geophys. Res. Lett.* **32**, L15709 (2005).
- [10] M. Paluš and D. Novotná, *Nonlinear Processes in Geophysics* **13**, 287 (2006).
- [11] U. Parlitz, L. Junge, W. Lauterborn, and L. Kocarev, *Phys. Rev. E* **54**, 2115 (1996).
- [12] N. F. Rulkov, M. M. Sushchik, L. S. Tsimring, and H. D. I. Abarbanel, *Phys. Rev. E* **51**, 980 (1995).
- [13] L. Kocarev and U. Parlitz, *Phys. Rev. Lett.* **76**, 1816 (1996).
- [14] M. G. Rosenblum, A. S. Pikovsky, and J. Kurths, *Phys. Rev. Lett.* **76**, 1804 (1996).
- [15] C. Schäfer, M. G. Rosenblum, J. Kurths, and H.-H. Abel, *Phys. Rev. E* **60**, 857 (1999).
- [16] R. Bartsch, J. W. Kantelhardt, T. Penzel, and S. Havlin, *Phys. Rev. Lett.* **98**, 054102 (2007).
- [17] M.-C. Wu and C.-K. Hu, *Phys. Rev. E* **73**, 051917 (2006).
- [18] D. Rudrauf, A. Douiria, C. Kovach, J.-P. Lachaux, D. Cosmellia, M. Chavez, C. Adama, B. Renault, J. Martinerie, and M. Le Van Quyen, *Neuroimage* **31**, 209 (2006).
- [19] N. E. Huang, Z. Shen, S. R. Long, M. C. Wu, H. H. Shih, Q. Zheng, N.-C. Yen, C. C. Tung, and H. H. Liu, *Proceedings: Mathematical, Physical and Engineering Sciences* **454**, 903 (1998).
- [20] M. Hoke, K. Lehnertz, C. Pantev, and B. Lütkenhöner, in *Dynamics of cognitive and sensory processing in the brain*, edited by E. Basar and T. Bullock (Springer, Berlin, Heidelberg, New York, 1988), pp. 84–105.
- [21] C. Allefeld and J. Kurths, *Int. J. Bif. Chaos* **14**, 406 (2004).
- [22] M. Paluš, *Physica D* **80**, 186 (1995).
- [23] S. Boccaletti, J. Kurths, G. Osipov, D. L. Valladares, and C. S. Zhou, *Phys. Rep.* **366**, 1 (2002).
- [24] M. Baptista, T. Pereira, and J. Kurths, *Upper bounds in phase synchronous weak coherent chaotic attractors*, *Physica D* **216**, 260 (2006).
- [25] E.-H. Park, M. A. Zaks, and J. Kurths, *Phys. Rev. E* **60**, 6627 (1999).
- [26] M. A. Zaks, E.-H. Park, M. G. Rosenblum, and J. Kurths, *Phys. Rev. Lett.* **82**, 4228 (1999).
- [27] A. Pujol-Peré, O. Calvo, M. A. Matías, and J. Kurths, *Chaos* **13**, 319 (2003).
- [28] A. S. Pikovsky, M. G. Rosenblum, and J. Kurths, *Int. J. Bif. Chaos* **10**, 2291 (2000).
- [29] W. H. Press, S. A. Teukolsky, W. T. Vetterling, and B. P. Flannery, *Numerical Recipes* (Cambridge University Press, Cambridge, 1992).
- [30] P. R. Bevington and D. K. Robinson, *Data Reduction and Error Analysis for the Physical Sciences* (McGraw-Hill, New York, 1992).
- [31] R. von Mises, *Mathematical Theory of Probability and Statistics* (Academic Press, New York, 1964).
- [32] P. Rousseeuw, *Journal of the American Statistical Association* **79**, 871 (1984).
- [33] P. Rousseeuw and K. van Driessen, *Computing lts regression for large data sets*, *Data Mining and Knowledge Discovery* **12**, 29 (2006), ISSN 1384-5810.
- [34] A. S. Pikovsky, M. G. Rosenblum, and J. Kurths, *Europhys. Lett.* **34**, 165 (1996).
- [35] M. G. Rosenblum, A. S. Pikovsky, and J. Kurths, *IEEE Trans. on Circuits and Systems* **44**, 874 (1997).
- [36] A. S. Pikovsky, G. Osipov, M. G. Rosenblum, M. Zaks, and J. Kurths, *Phys. Rev. Lett.* **79**, 47 (1997).
- [37] A. Stefanovska, H. Haken, P. V. E. McClintock, M. Hožič, F. Bajrović, and S. Ribarič, *Phys. Rev. Lett.* **85**, 4831 (2000).
- [38] F. Takens, in *Lecture Notes in Mathematics* (Springer, 1981), vol. 898, pp. 366–381.
- [39] T. Sauer, J. Yorke, and M. Casdagli, *J. Stat. Phys.* **65**, 579 (1991).
- [40] R. Quian Quiroga, T. Kreuz, and P. Grassberger, *Phys. Rev. E* **66**, 041904 (2002).

[41] If a negative trend exists, it will be converted to a positive trend by the procedure but the autocorrelation structure

will still be preserved.